

Original Article

Assembly of Portable Subsurface Penetrating Radar for the Concrete Delamination Assessment in the Surigao State College of Technology Building

Vrian Jay Ylaya¹, Gregorio Gamboa Jr², Robert Bacarro³, Mauricio Adlaon⁴, Emmylou Borja⁵
Rowena Plando⁶

¹Associate Professor of CEIT, Surigao State College of Technology, Surigao City, Philippines

²President, Surigao State College of Technology, Surigao City, Philippines

³Dean of CEIT, Surigao State College of Technology, Surigao City, Philippines

⁴VP RDE, Surigao State College of Technology, Surigao City, Philippines

⁵VP Academics, Surigao State College of Technology, Surigao City, Philippines

⁶VP Administration, Surigao State College of Technology, Surigao City, Philippines

¹vrianjayyaya@ssct.edu.ph, ²greggy3659@yahoo.com, ³rbacarro@ssct.edu.ph

Abstract -To protect the integrity and safety of buildings damaged by earthquakes, delaminated concrete must be inspected as soon as possible. On the other hand, a manual examination has limitations in determining the extent of internal concrete structural damage. This research aims to assemble a portable subsurface penetrating radar that can detect concrete delamination and assess it scientifically and quickly. The completed system was analyzed by building a concrete block with air pockets to simulate concrete delamination and scanning the block while watching the hyperbola fluctuation in the radargram. Actual scanning of the basketball court and the Surigao State College of Technology building found delaminated concrete. The integrated subsurface penetrating radar for concrete delamination demonstrates successful rapid assessment based on and actual site testing.

Keywords — Assembled System; Concrete Air Void; Delamination; Penetrating Radar; Radargram; Subsurface Penetrating Radar.

I. INTRODUCTION

In 2017, Surigao City was surprised 6.7 magnitude earthquake with total damage of 0.7 billion pesos, including houses, bridges, schools, roads, highways, public and private buildings, flood control structures, seaports, airports, and hospitals [1]. Philippine Trench continues to extend southward along the east side of Halmera-Palau's fault, which leads to the future frequent earthquake in the Caraga region [2]. A study of intervention and mitigation of the expected earthquake in terms of evacuation distance, tsunami alert, and facility damage was conducted where the facility damage influences the evacuation of choice in Surigao del

Norte[3]. Thus, the structural design of the building must be strong enough to withstand the ground shaking for refuge[4]. Assessment of the structures that survived the previous earthquake, especially public schools and bridges, was manually conducted using visual inspection and echo methods[5]. This method needs an expert to discern defects[6]. Still, the accuracy is limited[7]. Efficiency was improved using acoustic scanning in monitoring the condition of bridges[8]. Still, it suffered mobility and required more human resources to conduct the testing. Rapid detection of the crack in reinforced concrete structures using infrared thermography to improve mobility [9], but the assessment depended on the surrounding ambient temperature[9]. Subsurface detection using frequency modulated continuous wave FMCW radar using electromagnetic wave EM was also simulated [10]. Implementation of FMCW radar is low cost and portable but suffers sensitivity issues with limited penetration [11]. Ground-penetrating radar aims the improve penetration[12] and sensitivity but suffers portability and is expensive [13]. Due to the lack of a modular form of subsurface penetrating radar on the market[14], this study intends to assemble a subsurface penetrating radar to identify and capture delaminated concrete structures in the building using an EM wave. An assembled subsurface penetrating radar was finished. Experiments were conducted using simulated delaminated concrete, with field tests[15] proving that the device works.

II. THEORETICAL FRAMEWORK

This section illustrates the idea and scientific concept of impulse radiated signal and its behavior when applied to any solid object—generating impulse signal and processing the



reflected signal for interpretation to detect subsurface objects.

A. Theoretical Framework

Electromagnetic wave radar is also known as the electromagnetic reflection method[16]. The transmitting antenna (Tx) sends a wave into the structure being examined in the reflection mode, as shown in Figure 1. Because of discontinuities in the material, a part of the energy has reflected the radar. In contrast, part continues through the structure[17]. The reflected signal is recorded by the receiving antenna (Rx) and analyzed in a central unit. A discontinuity could be a boundary or interface between two materials with different dielectric properties or a subsurface object such as delamination or voids[18]. As shown in Figure 2 and the corresponding arrival times, the amplitudes of the detected echoes can then be used to locate the discontinuity.

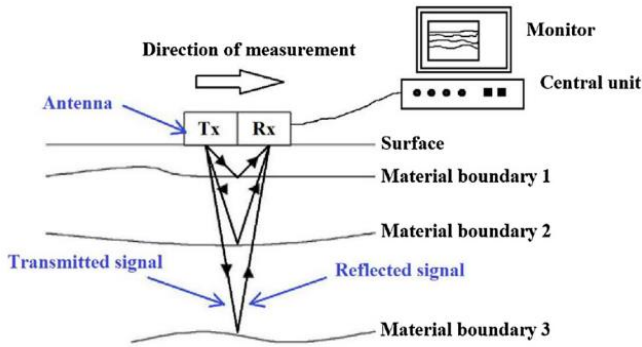


Fig 1 Principle of Radar Measurement[12]

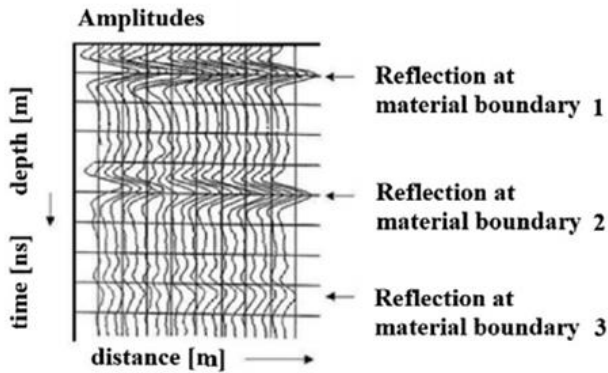


Fig 2 Radargram or B-scan [19]

The electromagnetic wave signal travels in one path (i.e., incident signal) to the material. Some of the signals are reflected (i.e., reflected), and some of the incident signals are piercing the material[20]. As illustrated in Equations (1) and (2), the behavior of incident and reflected energy is a function of transmission (T) and reflection coefficients (R), which are also reliant on the relative impedance (Z_r) of different materials. As demonstrated in Equation (3), the

relative impedance of the material is inversely proportional to the dielectric constant ($\epsilon_0\epsilon_r$) of the material[21].

$$R = \frac{Z_{r2} - Z_{r1}}{Z_{r2} + Z_{r1}} \text{ Equation(1)}$$

$$T = 1 - R \text{ Equaiton (2)}$$

$$Z_r = \sqrt{\frac{m_0}{\epsilon_0\epsilon_r}} \text{ Equation (3)}$$

$$\text{where } m_0 = \frac{4\pi \times 10^{-7} H}{m} = \text{magnetic permiability of free space}$$

As a result, the smaller the difference in dielectric constants between the two materials, the lower the reflection coefficient (R). This means that the change in amplitude of the energy or attenuation reflected from the interface of two different materials is a good indicator of their features. Consequentially, as the incoming signal travels and encounters various materials, other reflections are sent back to the antenna and recorded over time to build the waveform or radargram[22]depicted in Figure 2. Determining delamination or cavities in concrete is made more accessible by measuring the timing and amplitude of reflections in the waveform.

III. MATERIALS AND METHODS

The proposed assembled subsurface penetrating radar materials were composed of an antenna, radar module, software, and computer. The parts were bought separately since the aim of this project is to assemble subsurface penetrating radar. The system parts were carefully selected which the only target is delaminated concrete with a thickness of not more than 1m.

A. Antenna

The antenna used in the experiment was two Vivaldi as shown in Figure 3 with a frequency range of 1.3-4.4GHz, average gain up to 9.15dBi at a frequency of 3.4GHz, with an impedance of 50 ohms, size of 150x113x8mm, and voltage standing wave ratio (VSWR) of 2.1:1. Vivaldi was used in this experiment due to its compactness and high efficiency in transmitting and receiving capabilities [23].



Fig 3 Antenna

B. Radar Module

The transceiver module used was the RVS-M1, which is an ultra-wideband short-range radar PicoR-2k evaluation kit [24] with parameters such as a frequency range (at a level of -10dB) of 500MHz to 5GHz at a central frequency of 1200MHz/1600MHz, a pulse duration of 600ps, a pulse amplitude voltage of 6V, and a pulse repetition frequency of 50MHz, as shown in Figure 4. This module is utilized to measure the thickness of the ice and a sensor for motion detection [25].

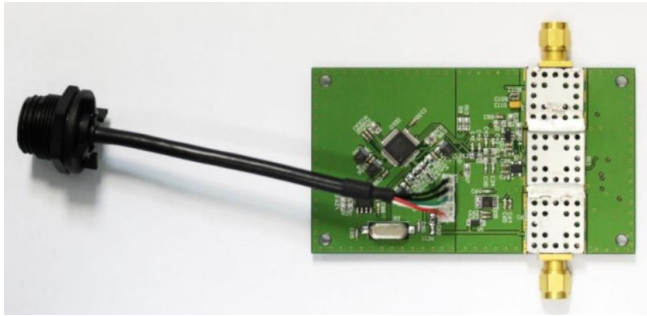


Fig 4 Transceiver Module

C. Software for Signal Processing

The transceiver was linked to a PC with 8GB of RAM, eight-core central processor units, a 6GB video card, and a 500GB solid-state drive [26]. This specification was sufficient for processing the radar signals [27], as depicted by the radargram in Figure 5. PicoR software was used to analyze and represent the radar signals that were broadcast and reflected. The radargram in the PicoR's GUI [28] was used to analyze the identified delaminated concrete; additionally, dielectric changes as the signal traveled to a different medium were noticed through the radargram [29].

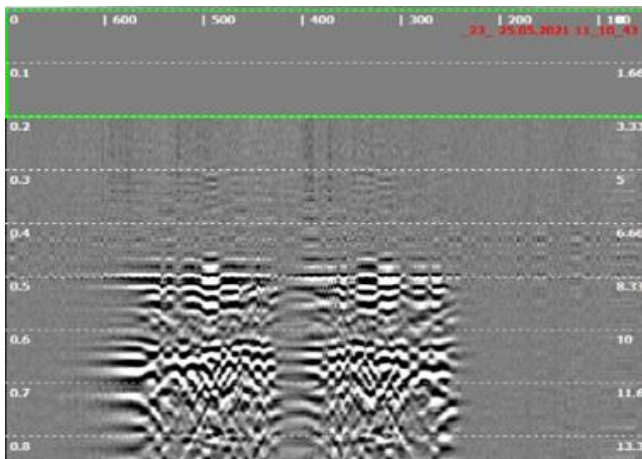


Fig 5 Radargram Analysis

D. Experimental Activity

The experiment was carried out with two specimens of concrete block and concrete block with void space to test the impulse radar capabilities in detecting the void space [27]. Figure 6 depicts one model that employs a purely concrete

block with dimensions of 6x100x100cm. Figure 7 depicts another specimen with a glass bottle mixed in a concrete block with dimensions of 6x100x100cm.



Fig 6 Concrete Block



Fig 7 With Space Void as Delaminated Portion

E. Surigao State College of Technology Building

As illustrated in Figure 10, the actual test was conducted at the Surigao State College of Technology-Main Campus. An experienced civil engineer conducted a visual investigation of the school site to identify locations of delaminated concrete, as shown in Figure 11.



Fig 10 Campus Map

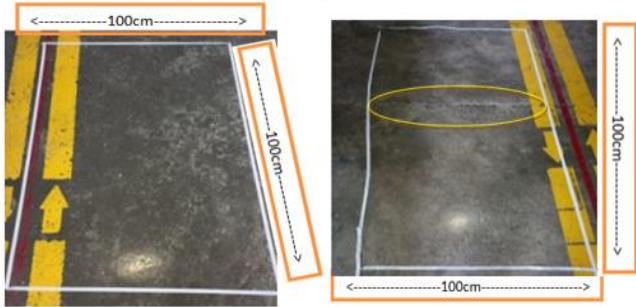


Fig 11 With and Without Delaminated Concrete

The area was chosen based on visual inspections conducted by the Surigao State College of Technology's resident civil engineer collaborating with the SSCT's Building and Estates team.

IV. RESULTS AND DISCUSSION

This section discusses the output of the completed set-up of assembled subsurface penetrating radar, scanning results, simulation results, pre, and actual testing results.

A. Complete Set-up

Figure 12 depicts the completed set-up of the assembled subsurface penetrating radar for delamination detection on a cart. The cart was designed to trial and error to determine the correct size to enhance signal transmission and use a plastic body to decrease ringing [26]. The antenna was placed closer to the ground to maximize signal transmission and reception.



Fig 12 Impulse Radar System

B. Scanning Procedure

As shown in Figure 13, an assembled subsurface penetrating radar was utilized to scan the specimen using one forward and one backward scan [30]. Every forward and backward movement of the scan is guaranteed to hit the target, and radargram results will be viewed in the personal computer for analysis and interpretation [31].

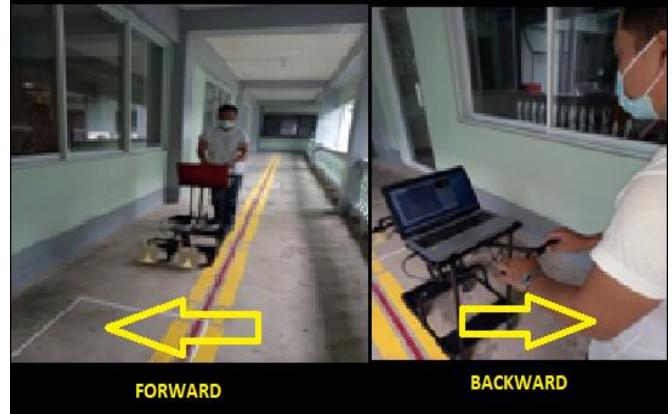


Fig 13 Scanning

C. Simulation Results

Figure 14 and Figure 15 specimens were now scanned and analyzed the radargram as shown in Figure 5.3a and Figure 5.3b. The radargram shows a flat and uniform hyperbolic properties because the concrete has distributed and constant dielectric properties, as shown in Figure 14.

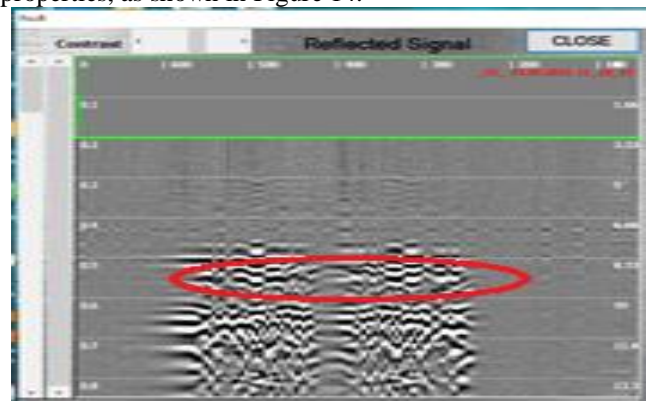


Fig 14 Radargram for concrete block

The radargram result of Figure 15 shows that the hyperbolic curve was evident because the air was present inside the concrete. Air has lesser dielectric property compared to concrete does it will disrupt the variation of signal reflections as observed in the radargram.

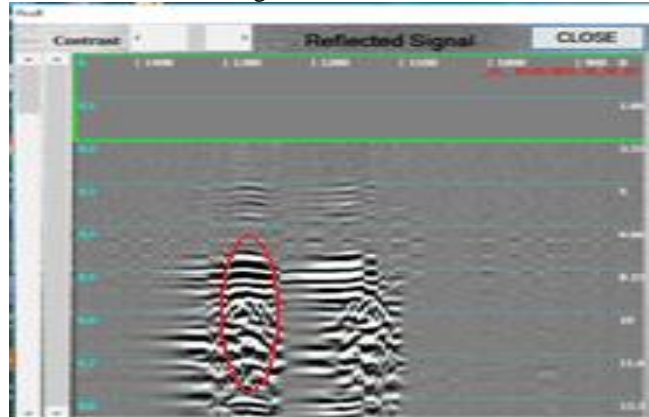


Figure 15. Radargram for Concrete with Void Inside

D. Pre-actual Testing Results

After the simulation results, the researcher now knows how the radargram behaves if space void or delamination were available in the concrete. The effects on the radargram of Figure 14 and Figure 15 are shown in Figure 16 and Figure 17. The contrast between the two demonstrates that the delaminated concrete generates stiff hyperbola due to air void or delamination when scanned.

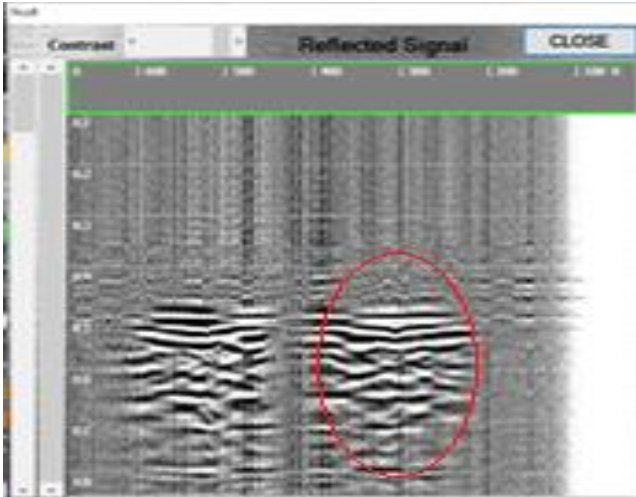


Fig 16 Without Delamination

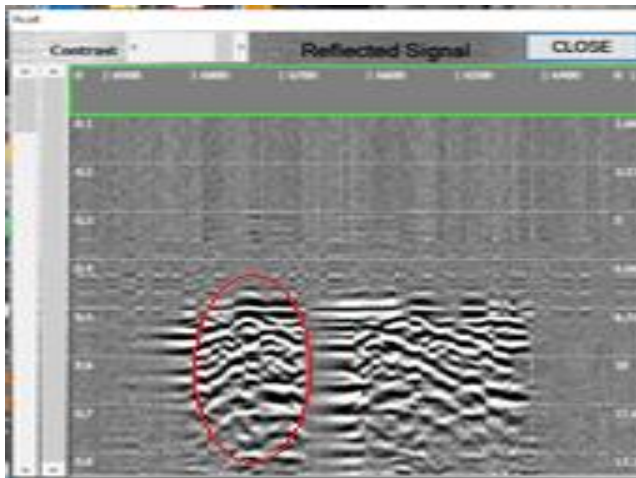


Fig 17 Delaminated Floor

E. Actual Testing Results

The impulse radar was tested on the actual setting on the old Surigao State College of Technology on the second floor, as shown in Figure 14. Inspection and selection of the floor were carefully selected by an experienced civil engineer of the campus, as shown in Figure 15.

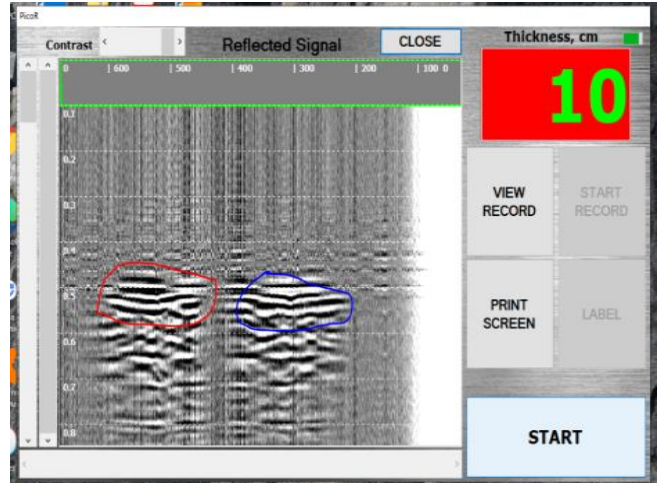


Fig 18 Without Delamination

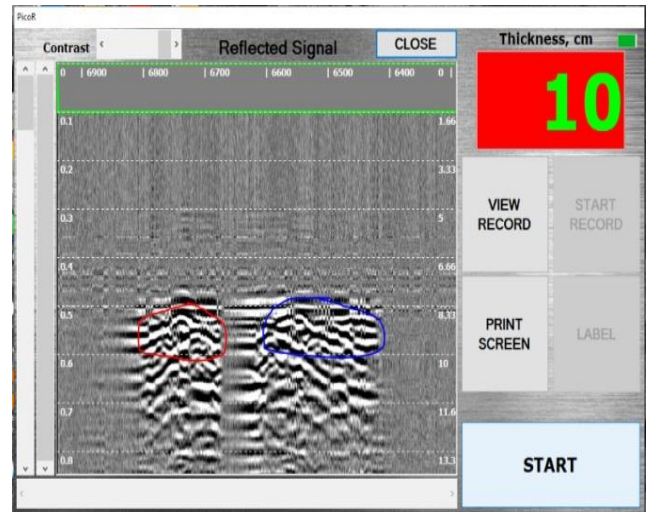


Fig 19 With Delaminated Floor

The radargram results of Figure 19 show the difference of with and without delamination. The system also estimated the thickness of the slab floor at 10cm, and the reflected signal also indicates a strong hyperbola form that represents the dielectric property of a space void or the delaminated part of the concrete.

VI. CONCLUSIONS

Antenna, radar module, software, and computer materials were effectively combined. The assembled subsurface penetrating radar system's ability to identify delaminated concrete was successfully tested. The subsurface penetrating radar analyzes the reflected signal from different dielectric materials, which results in a hyperbola on the radargram. The hyperbola is formed by dielectric changes, representing pure concrete and delaminated concrete, respectively. As a result of its radargram presentation, the assembled subsurface penetrating radar displays dependable results in detecting delaminated concrete.

REFERENCES

- [1] Louise JARDER, S., Estelito GARCIANO, L., & Francis... - Google Scholar.
https://scholar.google.com/scholar?hl=en&as_sdt=0%2C5&q=Louise+JARDER%2C+S.%2C+Estelito+GARCIANO%2C+L.%2C+%26+Francis+SISON%2C+F.+%282017%29.+Infrastructure+damage+during+the+Surigao%2C+Philippines+earthquake.&btnG= (2021).
- [2] R. K. Cardwell, B. L. Isacks, D. E. Karig., The spatial distribution of earthquakes, focal mechanism solutions, and subducted lithosphere in the Philippine and northeastern Indonesian Islands., *Tecton. Geol. Evol. Southeast Asian seas islands. Part 1*, (1980) 1–35.
- [3] Earthquake Evacuation Choice Models Based on the Stated Preference Approach for Residents in Surigao City, Philippines, *J. East. Asia Soc. Transp. Stud.*, 13 (2019) 70–79.
- [4] A. Pomonis, R. Spence, P. Baxter., Risk assessment of residential buildings for an eruption of Furnas Volcano, São Miguel, the Azores, *J. Volcanol. Geotherm. Res.*, 92(1–2) (1999) 107–131.
- [5] Y. Fujino, D. M. Siringoringo, Y. Ikeda, T. Nagayama, T. Mizutani., Research and Implementations of Structural Monitoring for Bridges and Buildings in Japan, *Engineering*, 5(6) (2019) 1093–1119.
- [6] S. Gholizadeh., A review of non-destructive testing methods of composite materials, in *Procedia Structural Integrity*, 1 (2016) 50–57.
- [7] G. K.-J. of C. Heritage and undefined, Using advanced NDT for historic buildings: Towards an integrated multidisciplinary health assessment strategy, Elsevier, Accessed: (2021).
- [8] K. Vaghefi et al., Evaluation of Commercially Available Remote Sensors for Highway Bridge Condition Assessment, *J. Bridg. Eng.*, 17(6) (2012) 886–895.
- [9] M. Bojan, B. I.- Zagreb, and undefined, The Role of Infrared Thermography in Nondestructive Testing of Civil Engineering Structures, *ib. irb.hr*, (2021).
- [10] J. M. S. MacAsero, O. J. L. Gerasta, D. P. Pongcol, V. J. V. Ylaya, A. B. Caberos., Underground target objects detection simulation using FMCW radar with SDR platform, 2018 IEEE 10th Int. Conf. Humanoid, Nanotechnology, Inf. Technol. Commun. Control. Environ. Manag. HNICEM 2018, (2019).
- [11] D. Pongcol, O. G., 2019 19th, and undefined 2019, Frequency Shift Keying Radar for Ground Object Detection in GNU-Radio with USRP, *ieeexplore.ieee.org*, (2021).
- [12] V. Ferrara et al., Design and Realization of a cheap Ground Penetrating Radar Prototype @ 2.45 GHz, 2016 10th Eur. Conf. Antennas Propagation, EuCAP 2016, (2016).
- [13] C. Le Bastard, V. Baltazart, Y. W.-I. T. on, and undefined., Thin-pavement thickness estimation using GPR with high-resolution and superresolution methods, *ieeexplore.ieee.org*, (2021).
- [14] F. Lombardi, M. Lualdi, F. Picetti, P. Bestagini, G. Janszen, L. A. Di Landro., Ballistic Ground Penetrating Radar Equipment for Blast-Exposed Security Applications, *Remote Sens*, 12(4) (2020) 717.
- [15] L. Pajewski, S. Fontul, M. Solla., Ground-penetrating radar for the evaluation and monitoring of transport infrastructures, *Innov. Near-Surface Geophys*, (2019) 341–398.
- [16] B. Ursin., Review of elastic and electromagnetic wave propagation in horizontally layered media, 48(8) (2012) 1063–1081.
- [17] M. Jankü, P. Cikrle, J. Grošek, O. Anton, J. Stryk., Comparison of infrared thermography, ground-penetrating radar and ultrasonic pulse-echo for detecting delaminations in concrete bridges, *Constr. Build. Mater*, 225 (2019) 1098–1111.
- [18] S. Kashif Ur Rehman, Z. Ibrahim, S. A. Memon, M. Jameel., Nondestructive test methods for concrete bridges: A review, *Constr. Build. Mater*, 107 (2016) 58–86.
- [19] W. Wai-Lok Lai, X. Dérobert, P. Annan., A review of Ground Penetrating Radar application in civil engineering: A 30-year journey from Locating and Testing to Imaging and Diagnosis, *NDT E Int.*, 96 (2018) 58–78.
- [20] D. Kahn., *Earth Sound Earth Signal, Earth Sound Earth Signal*, (2020).
- [21] M. H. Abdullah, A. N. Yusoff., Complex impedance and dielectric properties of an Mg□Zn ferrite, *J. Alloys Compd*, 233(1–2) (1996) 129–135.
- [22] E. Slob, M. Sato, and G. Olhoeft, Surface and borehole ground-penetrating-radar developments, 75(5) (2010).
- [23] D. N. Elsheakh, E. A. Abdallah., Compact ultra-wideband Vivaldi antenna for ground-penetrating radar detection applications, *Microw. Opt. Technol. Lett.*, 61(5) (2019) 1268–1277.